Text to supplementary supplement Figure 1

In the expression profiling screen, upregulation of PDGF signaling pathway components included the PDGFR downstream target STAT1, (1), which is known to be activated in breast cancer (1, 2). In this screen, Stat1 mRNA was upregulated in a strictly EMT /metastasis-specific fashion (Figure 1A; (2). We therefore confirmed strong expression of STAT-1α/β proteins in EpRasXT cells, but not in EpRas cells before EMT (Figure S1A). PDGF activates STAT proteins in EpRasXT cells but not in EpRas cells, as analysed by EMSA (Figure S1B, C). PDGF-treatment of mesenchymal EpRasXT and EpS35-XT cells strongly enhanced DNA binding of STAT-1, while PDGF failed to activate STAT-1 in EpC40-XT cells, or in epithelial EpRas, EpS35 or EpC40 cells (Figure S1C, see Figure 1A). Therefore, both STAT1 expression and its activation by PDGF occurs in a strictly EMT-specific fashion, which is consistent with a role of STAT1 during tumor progression.

Legend to supplement Figure 1.

Autocrine PDGFR signaling upregulates and activates STAT1 in an EMT-specific fashion

Total levels of STAT1 in extracts from Ep-Ras and EpRasXT cells were determined by Western Blot, using antibodies to Smad2/3 as a loading control. **C**: EpRasXT cells were treated with PDGF (+) or left untreated (-) and nuclear extracts processed for Stat1/3 DNA binding (EMSA), using antibodies known to supershift STAT1 and STAT 3α to identify STAT-DNA complexes. **D**: EpH4 cells and respective derivatives were lysed before and after inducing EMT (EpRas, EpS35) or scattering (EpC40) and subjected to DNA-binding analysis for STAT1/3.

Text to supplement Figure 2

Our observation that EpRas cells expressing a dominant-negative PDGF-receptor (EpRas-dnP) failed to undergo EMT in collagen gels upon treatment with TGFβ (Figure 6B), in contrast to EpRas-GFP-induced control cells, strongly suggested a more detailed characterisation of the respective tumors formed by these cells in nude mice for EMT in vivo. Staining for Vimentin and E-cadherin demonstrated, that EpRas-dnP cells still expressed delocalized E-cadherin, sometimes clearly at the plasma membrane, while these cells were negative for the mesenchymal marker vimentin. In contrast, cells from EpRas-GFP induced tumors did undergo EMT, since they expressed vimentin, but not E cadherin (Figure S2, top- and middle panels), similarly as published previously (3). Since essentially all tumor cells from both cell types were also positive

for basal cytokeratins (Figure S2, bottom panels), it is very unlikely that the vimentin positive, E cadherin negative cells from the EpRas-GFP tumors represent stromal cells, which do not express cytokeratins (3). In both tumor types, the vimentin antibody stained the (mesenchymal) capsule (3) around the tumors, which was negative with the E-cadherin antibody. In conclusion, dnP inhibits EpRas cells from undergoing EMT also in mouse tumors.

Legend to supplement Figure 2

EpRas-dnP cells are tumorigenic but fail to undergo EMT when injected into the mammary fat pad

Tumors formed from EpRas-dnP cells (left panels) or EpRas-GFP control cells (right panels) were subjected to cryosectioning and subsequently staining with antibodies to Vimentin (top), E-Cadherin (middle) and Cytokeratin (bottom, see Materials and Methods). For each antibody staining, several regions from the tumor interior and (where indicated) one region from the tumor edge are shown. Original magnification, x40

Text to supplement Figure 3

Besides staining for epithelial and mesenchymal markers, we also analysed tumor histology, using cryosections from formaldehyde fixed and then frozen tumors (explaining the suboptimal conservation of the tissues). Nevertheless, it can be seen, that the EpRas-GFP induced tumors consist of spindle-like, nonadherent cells forming a loose meshwork, whereas the EpRas-dnP tumor cells were less spindle-like and formed regions of more tightly packed, less spindle-like cells. This corresponds well to the morphology of the cells in respective collagen gel structures (main text, Figure 5B, top group of panels).

Legend to supplement Figure 3 *Histology of tumors induced by EpRas-dnP and EpRas GFP.*

Cryosections from tumors formed by EpRas-dnP cells (left panels) or EpRas-GFP control cells (right panels) are shown after HE-staining. Insets show typical regions from the tumors at higher magnification. Note abundant blood vessels (orange) in the EpRas-dnP tumors. Original magnification, x20 , x100 (inserts)

Text to supplement Figure 4

The human mammary carcinoma cell lines MDA-MB-231 and CAMA-1 exhibit a mesenchymal phenotype characterized by loss of E-cadherin and high expression of vimentin and the E-

cadherin repressor delta EF-1 (4). Cultivation in collagen gels revealed formation of disordered, migratory cell structures by both cell types (Figure S4 A, B, controls). A specific PDGFR-tyrosine kinase inhibitor (see Materials and Methods) interfered with the migratory phenotype of CAMA-1 cells, leading to more compact structures.

No such effect was seen on control cells (CT-26) which do not show elevated PDGFR-signaling upon EMT. The established cancer drug STI571 induced essentially complete cell disintegration in both MDA-MB-231 and CAMA-1 cells (Figure S4B), even at concentrations lower than those still fully tolerated by the CT26 control cells (0.4 instead of 1 uM, see insets in Figure S4B). In conclusion, both STI571 and the more specific tyrosine kinase inhibitor induced either apoptosis or loss of a migratory phenotype in human mammary carcinoma cell lines. These experiments have been performed in 3D collagen gels (recently reviewed in (5) under defined media conditions that would not provide enough PDGF for dependent cells to survive. Therefore, survival of CAMA1 and MDA-MB-231 cells that have not been treated with PDGFR tyrosine inhibitors (control structures) is consistent with these cell-lines apparently secreting PDGF themselves.

Legend to supplement Figure 4

Analysis of pharmacological PDGFR tyrosine kinase inhibitors on human mammary carcinoma cell lines with an EMT phenotype. **A**. CAMA-1 cells seeded into collagen gels (see Supplementary Material and Methods) for 4-5 days were exposed to a specific PDGFR tyrosine kinase inhibitor for 9-10 consecutive days and photographed. As a control, murine CT-26 colon carcinoma cells were treated with inhibitor in the same fashion. Note loss of migratory cells in the CAMA-1 cells but not in the CT-26 control. **B**. CAMA-1 and MDA-MB-231 cultivated in collagen gels for 5 days were exposed to STI571 in the concentrations indicated for another 8 days and photographed. We observed cell death with CAMA-1 and MDA-AB-231 cells at all concentrations tested (1μM and 0.4 μM). At the same time, these concentrations fully permitted survival, proliferation and migration of CT26 control cells. In case of low structure density, panels show several photographs from the same gel (separated by gray lines/squares). Original magnification, x20

Supplement to Materials and Methods

Detailed description of cells:

EpH4 cells, a murine mammary epithelial cell line spontaneously immortalized from midpregnant mice, retains complete epithelial polarization on porous supports but not on standard tissue culture plastic. In 3D serum-free collagen I gels, EpH4 cells form organotypic, tubular structures, which makes them particularly well suited to study epithelial cell plasticity (6-8).

EpH4 cells expressing oncogenic Ras (**EpRas**) formed tubular, branched structures of fully polarized cells, but EpRas cells showed faster growth, larger lumina as well as alveolar structures. We refer to this EpRas phenotype as plastic epithelium, to highlight their increased epithelial plasticity and migratory capacity, also observed in Ras-transformed kidney- and liver-derived cell systems (3, 9, 10).

Scattering and EMT are two phenotypical changes, both inducible in the same, clonal EpRas cells. Importantly, both phenotypes show similar loss of epithelial polarity, fibroblastoid morphology and enhanced motility. They can, however, be distinguished by marker gene analysis and reversibility studies.

Scattering is fully reversible after removal of the inducing factors, epithelial markers are redistibuted but not lost, and mesenchymal markers (e.g. vimentin) are not induced. Scattering is induced by FGF, HGF (in EpRas or EpH4 cells) or TGFβ (in apoptosis protected EpH4),the latter requiring protection from apoptosis by potent survival signals like Bcl2 overexpression or activation of the PI3K-pathway (11).

In contrast, *EMT* persists after removal of inducing signals and involves loss of epithelial markers and expression of mesenchymal markers such as vimentin (3, 12, 13). Typically, EMT-inducing signal combinations involve oncogenic Ras and TGFβ, which have to act on the cells for prolonged time periods (>4-6 days, (3, 9, 10, 14)). In both 3D cultures and in tumorigenesis, EMT requires autocrine TGFβ secretion, which maintains EMT as a metastable phenotype independently of exogenous factors (3, 7, 11).

EpS35 and EpC40 cells: To dissect Ras-downstream signaling with respect to EMT, two Ras effector-specific mutants (15) which predominantly signal either through the ERK/MAPK pathway (S35-V12Ras) or through the PI3K-PKB/AKT pathway (C40-V12Ras) were expressed in polarized mammary epithelial cells (EpH4). Exposure of these cells to TGFb demonstrated that EMT requires hyperactivation of the ERK/MAPK pathway by S35-Ras, while hyperactive PI3K signaling induced by Ras-C40 enabled TGFb-induced ‘scattering’ in EpH4 cells, a distinct

fibroblastoid, migratory phenotype without persistent expression changes in epithelial or mesenchymal markers (11, 16). In addition, Ras-C40 induced protection from TGFβ-induced apoptosis and hyperproliferation in 3D collagen gel culture, similar to Ras with an unmutated effector loop, while Ras-S35 caused only moderate apoptosis protection and no hyperproliferation. TGFb-induced scattering is also observed in EpH4 cells protected from apoptosis by overexpression of the antiapoptotic protein Bcl-2 (11). Injection of the above cells into nude mice showed that hyperactivation of the ERK/MAPK or PI3K pathway but not Bcl-2 overexpression was sufficient to render EpH4 cells tumorigenic. Importantly, metastasis formation required EMT induced by TGF□ plus a hyperactivated ERK/MAPK pathway (11). including key regulators of cell proliferation and survival, epithelial polarity and motility/invasiveness.

The murine **CT26 cell line**, derived from a chemically induced carcinoma (17) is highly tumorigenic in syngeneic or nude mice. CT26 cells expressing dnTGFbeta-receptor (**CKR cells**) fail to invade 3D collagen gels and to metastasise in tail vain injection assays using nude mice (7).

The human mammary carcinoma cell lines **CAMA-1 and MDA-MB-231** were selected from a collection of ≈ 20 human mammary carcinoma lines by mesenchymal morphology, complete loss of E-cadherin expression and high expression of the E-cadherin repressor delta-EF-1 (4). MDA-MB-231 was also shown to express vimentin and to regain E cadherin expression upon knockdown of delta EF-1 by RNAi (4).

Collagen gel culture and marker analysis

Serum free, 3D cultures of Ep-Ras cells and their derivatives were described earlier (3, 4). TGFβ (5 ng/ml), α-PDGF neutralizing antibody (αPDGFA/αPDGFB; Upstate Biotechnology (Upstate USA, Inc.); 20μg/ml) and control antibodies (goat- and bovine IgG, Sigma-Aldrich, 20μg/ml) were added to the cultures after 2-5 days, and then supplied together with fresh medium every other day, for a total of 5-7 days. An experimental, low molecular weight, specific PDGFR tyrosine kinase inhibitor (PDGFR-inhibitor) from Boehringer Ingelheim GmbH (2 μM), the drug STI571 (1 μM) and the PI3K inhibitor LY294002 were used. For TUNEL assays in collagen gels, cell structures were treated with the respective agents for 4 days. Collagen gels were fixed in 4 % PFA/PBS, washed 3x with PBS, and stained for apoptotic nuclei according to the

suppliers instructions for the Cell Death Assay Kit (F. Hoffmann-La Roche Ltd). In situ confocal immuno-fluorescence analysis was performed to analyse 3D structures for E-cadherin, vimentin, Calgranulin A/MRP8 and CD68 as described in (4). For quantification of the TUNEL assay >300 cells from 3 fields in each collagen gel were counted and average apoptotic indices determined from 2 collagen gels.

Cultivation of CAMA-1 and MDA-MB in collagen gels

MDA-MB-231 cells (2500 /gel) and CAMA-1 cells (3000/gel) were seeded into collagen gels as described earlier (11), except that 2% foetal calf serum was added to the otherwise unaltered medium. After 48 -72 hours (depending on initial structure formation) the structures were grown the serum was lowered to 0.25% for the remaining culture period. These conditions provide far less PDGF and other growth factors than needed for growth of PDGF dependent cells. For this reason TGFα and other supplements are added in a controlled fashion to the media like usual (details see 18). Inhibitors were added every second day at the final concentrations indicated.

Generation of dnPDGF-R expressing EpRas clones:

primers: forward AAAAAGCAGGCTTGATGGGGACCTCCCACC, reverse AGAAAGCTGGGTAGGATCCCAAAATCCGACC. The resulting fragment was further amplified with attB1:GGGGACAAGTTTGTACAAAAAAGCAGGCT and attB2:GGGGACCACTTTGTA-CAAGAAAGCTGGGT primers to yield a Gateway-vector-compatible fragment, that was cloned into pBABE-RFB-GFP vector to produce a dnPDGF- c-terminal GFP fusion protein.

Inhibitors:

An experimental, low molecular weight, specific PDGF-R tyrosine kinase inhibitor (PDGFR-inhibitor) from BI was used at 2μM, completely inhibiting PDGF-induced proliferation of primary human fibroblasts at 2-5μM with no inhibition of EGFR, HER2, IGF1-R, FGF-R, v-src, and numerous serine/threonine kinases, including TGFβRII kinase (G. Loeber, unpublished). The drug STI571 (Gleevec) was extracted from ground tablets in DMSO (stock 1 mM) and used at 1 μM. Dosage and application of the PI3 kinase inhibitor LY294002 has been described at (11).

Antibodies and equipment for In situ confocal immuno-fluorescence analysis:

The following antibodies were used: α-E-cadherin (Becton, Dickinson and Co., 610182); α-vimentin, Vim-13.4 (Sigma, cat# V-2258), α-CD68 (Santa Cruz Biotechnology Inc., sc-7084) and α-Calgranulin A/MRP8 (Santa Cruz Biotechnology Inc., sc-20174). Dapi (0.1 ng/ml) was used for nuclear counterstaining. Antibodies for analysis of formaldehyde-fixed, frozen tumor sections were: α-E-cadherin, same as above, Vimentin, Vim 13.2 (Sigma-Aldrich com, cat# V-5255), Cytokeratin, TROMA-1 from Developmental Studies Hybridoma bank (DSHB), University of Iowa, Dept. of Biological Sciences, Iowa City, IA 52242, USA Digital images were collected either on a Leica Confocal Microscope or with a MicroMax camera on a Zeiss Axioplan 2 using Micromorph software. Processing of digital images was done using Adobe Photoshop 7.0.

Antibodies for Western-Blot analyses:

Erk1/2 and phospho-Erk1/2 from Sigma-Aldrich; AKT and phospho-AKT from Cell Signaling Technology, Inc; RGFP from Gibco; STAT1 (M22) from Santa Cruz Biotechnology Inc; Smad 2/3 from BD Transduction Laboratories.

Electrophoretic mobility shift assay (EMSA)

Whole cell extracts were prepared by cell lysis in buffer containing 20mM Hepes (pH 7.9), 400mM NaCl, 1 mM EDTA, 20% glycerol, 1mM DTT, 1mM phenylmethylsulfonyl fluoride, 5μg/ml leupeptin, 0.2units/ml aprotinin, 5mM sodium ortho-vanadate, 1mM NaF, 5mM Glyerophosphate, followed by 4 freeze-thaw cycles. Extracts were cleared by centrifugation at 20,000 g for 30 min at 4°C and protein concentration determined (Bradford reagent; Biorad). For analysis of STAT1/STAT3 complexes, the SIEm67 STAT binding site from the human c-fos promoter was used as a probe. Double stranded blunt ended oligonucleotides (5'-CATTTCCCGTAAATC-3') were annealed and end-labelled [32P]-γ-ATP) to a specific activity of 10.000 cpm/fmol. Binding reactions were performed by incubating 10,000 cpm of radiolabelled probe with 20 μg of cell lysate for 30 min at room temperature. For supershift reactions of STAT containing complexes, 0,2 μg of antibodies to STAT1 (M22; Santa Cruz

Biotechnology Inc.), STAT3 (c-20; Santa Cruz Biotechnology Inc.) were added to the binding reactions before EMSA was performed (electrophoresis through 6% native polyacrylamide gels and autoradiography using BioMax sensitive films; Kodak).

Tumorigenesis and metastasis assays

Athymic MF1 nude mice (6-10 weeks old) were used for mammary gland- and tail vein injections as described previously (4). Mice were sacrificed at a tumor size of 1.5 cm. Tumors were excised, weighed and frozen in Tissue-Tek (Sakura). When indicated, mice were fed with a gavage one day before tail vein injection, and with STI571 (10mg/ml stock solution in DMSO; 0.1 mg/g body weight) for 6 consecutive days. The mice of an entire experiment were sacrificed at the time where control mice started to die from lung metastasis. Lungs were excised and weighed. To recultivate donor cells from lungs, the left half of the lung was minced, centrifuged and resuspended in 1 ml PBS, mixed with 1 ml 10x trypsin and incubated for 30 min at 37 C. Cells were washed once in 10 ml DMEM 10% FCS and seeded in 10 cm cell culture dishes plus 10 ml DMEM 10% FCS. Donor cells were selected with the appropriate antibiotic for 3 days and then subjected to FACS analysis. For histological analysis the entire lung or the right half were treated as described earlier (4). Total numbers of metastases per lung were determined by collecting serial lung sections, at distances of approximately 0.3 mm.

Tissue samples and Immunohistochemistry

Breast progression tissue microarrays included 16 normal mammary gland, 45 intraductal mammary carcinomas, and 93 invasive mammary carcinomas. Monoclonal antibodies against the extracellular domains of human PDGF receptor alpha (clone 35248) and PDGF receptor beta (clone PR7212) were obtained from R&D Systems (Minneapolis, MN). Breast tissue microarrays were pre-treated with Decloaker in 1x Reveal solution, and then incubated at 4C for one hour with PDGF receptor alpha at 15ug/ml or PDGF receptor beta at 25ug/ml, diluted in Tris-buffered saline. Biotinylated secondary antibodies (VectaStain ABC Kit, Vector) were then applied as per instructions and the reaction developed using diaminobenzidene for 5 minutes. The slides were subsequently rinsed with both tap and distilled H20 and counterstained with hematoxylin for analysis and scoring.

Primers for Quantitative RT-PCR

5´-TGGGTCCCATGCCATTAA -3', 5´- TCAATACTTCTCTTCCTGCGAA -3´), and 5´-Fam-TGTGCCCGAGAAGCGGCCT-Tamra-3´ for mouse PDGF-A; 5´-TCCGTGAGAACCAGCAGAG-3', 5´-AGACAGGCACCCTGTTTCAG -3´, and 5´-Fam-CTCCTGCCTAACTGAGCCTCAACCTC-Tamra-3´ for mouse PDGF-B or 5´-AACCAAATGAGATCAGAACCTACAA -3', 5´-TGTGGAA-AAGGTAGTGGAT GC -3´, and 5´-Fam-TTTGAATGTGAAGTTGACCCGTAAATCTGA-Tamra-3´ for mouse JE/MCP-1. As reference samples, both mouse 18S-RNA and GAPDH were employed, using respective Perkin Elmer control reagents.

Supplementary references

1. Heldin, C.H., and Westermark, B. 1999. Mechanism of action and in vivo role of platelet-derived growth factor. *Physiol Rev.* 79:1283-1316.
2. Buettner, R., Mora, L.B., and Jove, R. 2002. Activated STAT signaling in human tumors provides novel molecular targets for therapeutic intervention. *Clin Cancer Res* 8:945-954.
3. Oft, M., Peli, J., Rudaz, C., Schwarz, H., Beug, H., and Reichmann, E. 1996. TGF-beta1 and Ha-Ras collaborate in modulating the phenotypic plasticity and invasiveness of epithelial tumor cells. *Genes Dev* 10:2462-2477.
4. Eger, A., Aigner, K., Sonderegger, S., Dampier, B., Oehler, S., Schreiber, M., Berx, G., Cano, A., Beug, H., and Foisner, R. 2005. DeltaEF1 is a transcriptional repressor of E-cadherin and regulates epithelial plasticity in breast cancer cells. *Oncogene*.
5. Debnath, J., and Brugge, J.S. 2005. Modelling glandular epithelial cancers in three-dimensional cultures. *Nat Rev Cancer* 5:675-688.
6. Fialka, I., Schwarz, H., Reichmann, E., Oft, M., Busslinger, M., and Beug, H. 1996. The estrogen-dependent c-JunER protein causes a reversible loss of mammary epithelial cell polarity involving a destabilization of adherens junctions. *J Cell Biol* 132:1115-1132.
7. Oft, M., Heider, K., and Beug, H. 1998. TGFbeta signaling is necessary for carcinoma cell invasiveness and metastasis. *Current Biology* 8:1243-1252.
8. Reichmann, E., Schwarz, H., Deiner, E.M., Leitner, I., Eilers, M., Berger, J., Busslinger, M., and Beug, H. 1992. Activation of an inducible c-FosER fusion protein causes loss of epithelial polarity and triggers epithelial-fibroblastoid cell conversion. *Cell* 71:1103-1116.
9. Lehmann, K., Janda, E., Pierreux, C.E., Rytomaa, M., Schulze, A., McMahon, M., Hill, C.S., Beug, H., and Downward, J. 2000. Raf induces TGFbeta production while blocking its apoptotic but not invasive responses: a mechanism leading to increased malignancy in epithelial cells. *Genes Dev* 14:2610-2622.
10. Gotzmann, J., Huber, H., Thallinger, C., Wolschek, M., Jansen, B., Schulte-Hermann, R., Beug, H., and Mikulits, W. 2002. Hepatocytes convert to a fibroblastoid phenotype

through the cooperation of TGF-beta1 and Ha-Ras: steps towards invasiveness. *J Cell Sci* 115:1189-1202.

11. Janda, E., Lehmann, K., Killisch, I., Jechlinger, M., Herzig, M., Downward, J., Beug, H., and Grunert, S. 2002. Ras and TGF[beta] cooperatively regulate epithelial cell plasticity and metastasis: dissection of Ras signaling pathways. *J Cell Biol* 156:299-313.
12. Sun, D., Baur, S., and Hay, E.D. 2000. Epithelial-mesenchymal transformation is the mechanism for fusion of the craniofacial primordia involved in morphogenesis of the chicken lip. *Dev. Biol.* 228:337-349.
13. Hay, E.D. 1995. An overview of epithelio-mesenchymal transformation. *Acta Anat (Basel)* 154:8-20.
14. Cui, W., Fowlis, D.J., Bryson, S., Duffie, E., Ireland, H., Balmain, A., and Akhurst, R.J. 1996. TGFbeta1 inhibits the formation of benign skin tumors, but enhances progression to invasive spindle carcinomas in transgenic mice. *Cell* 86:531-542.
15. Rodriguez-Viciana, P., Warne, P.H., Khwaja, A., Marte, B.M., Pappin, D., Das, P., Waterfield, M.D., Ridley, A., and Downward, J. 1997. Role of phosphoinositide 3-OH kinase in cell transformation and control of the actin cytoskeleton by Ras. *Cell* 89:457-467.
16. Grunert, S., Jechlinger, M., and Beug, H. 2003. Diverse cellular and molecular mechanisms contribute to epithelial plasticity and metastasis. *Nat Rev Mol Cell Biol* 4:657-665.
17. Brattain, M.G., Strobel-Stevens, J., Fine, D., Webb, M., and Sarrif, A.M. 1980. Establishment of mouse colonic carcinoma cell lines with different metastatic properties. *Cancer Res* 40:2142-2146.
18. Janda, E., Litos, G., Grunert, S., Downward, J., and Beug, H. 2002. Oncogenic Ras/Her-2 mediate hyperproliferation of polarized epithelial cells in 3D cultures and rapid tumor growth via the PI3K pathway. *Oncogene* 21:5148-5159.

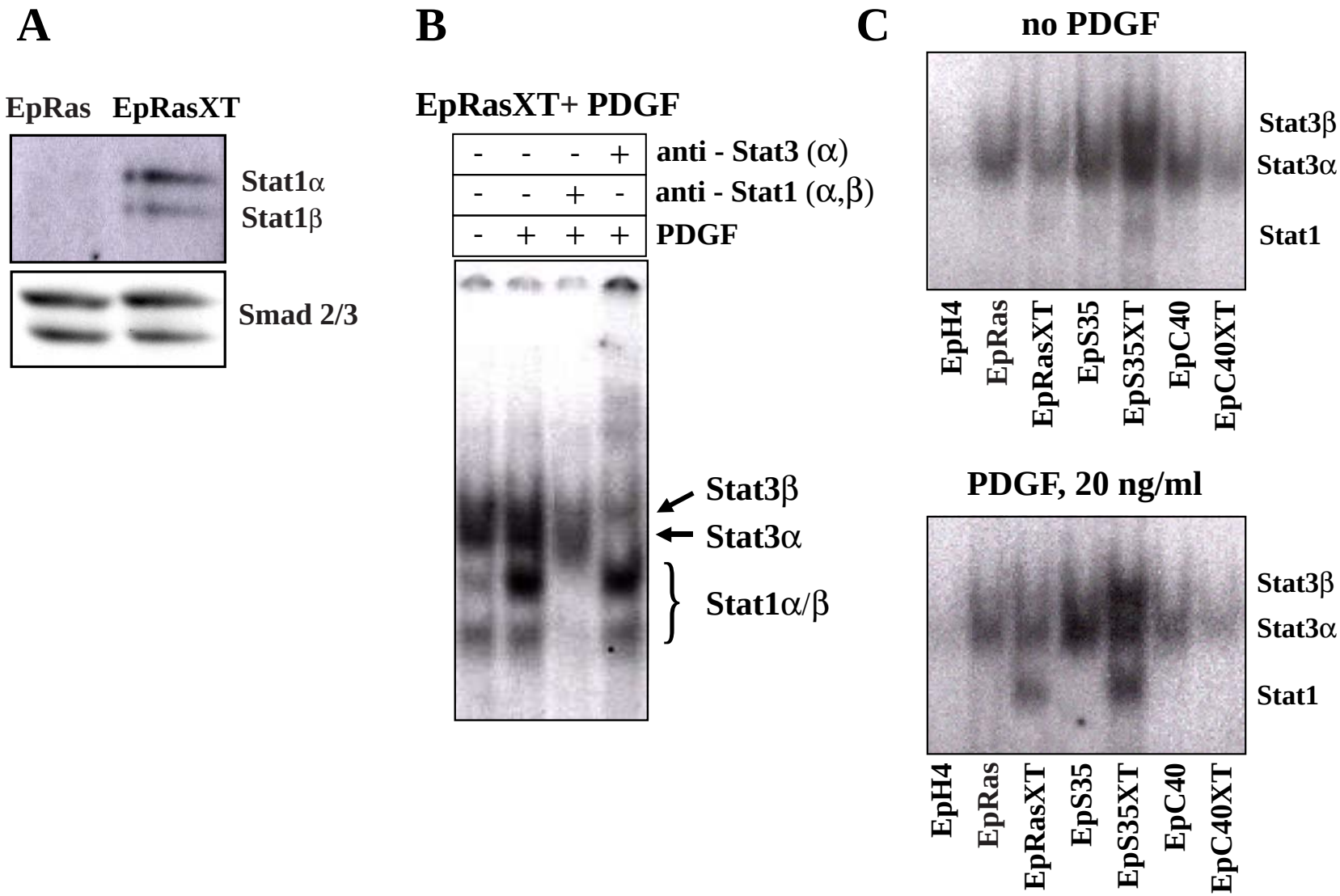

Jechlinger et al., Fig. S1

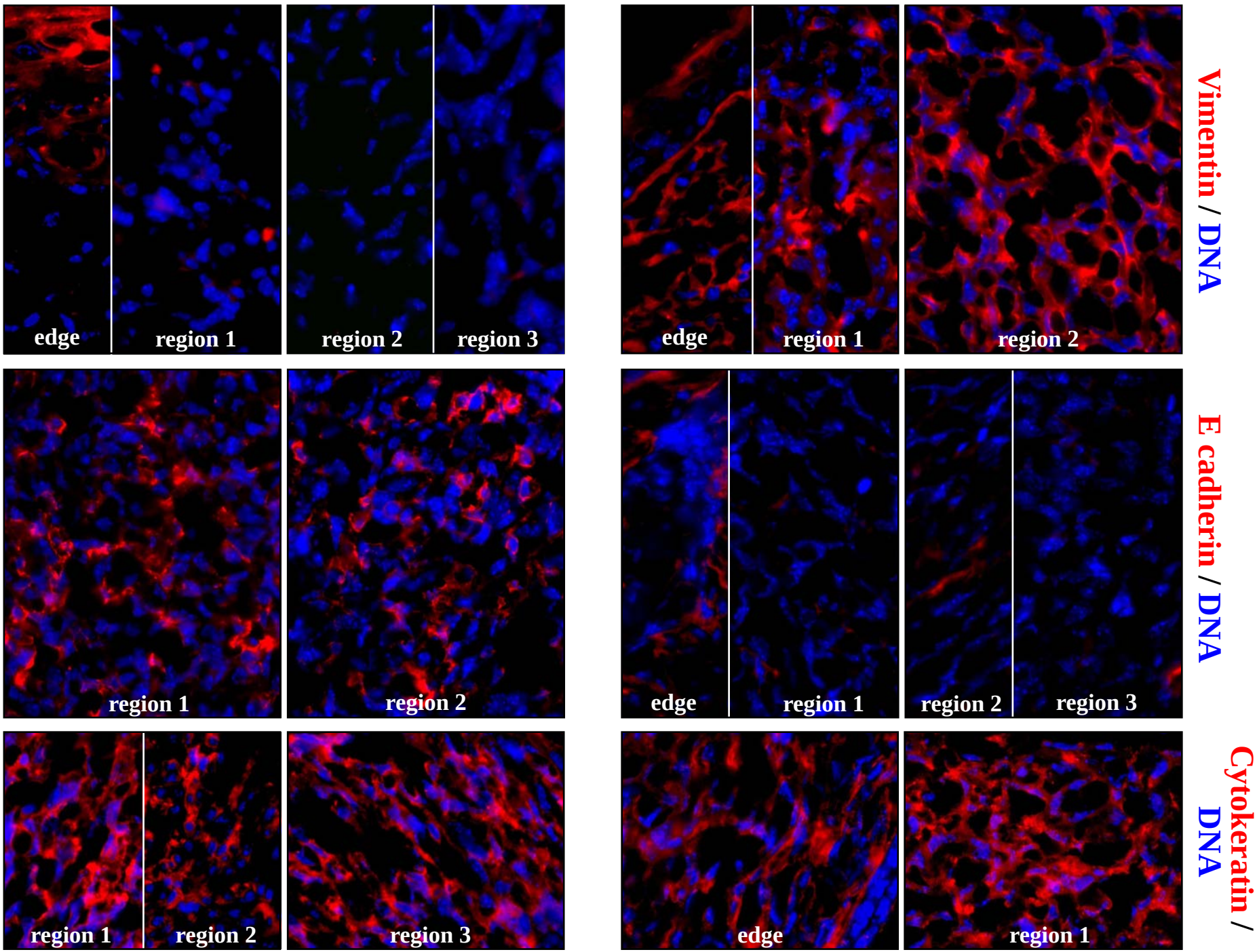

Jechlinger et al., Fig. S2

EpRasXT-GFP- dnP

EpRasXT-GFP-control

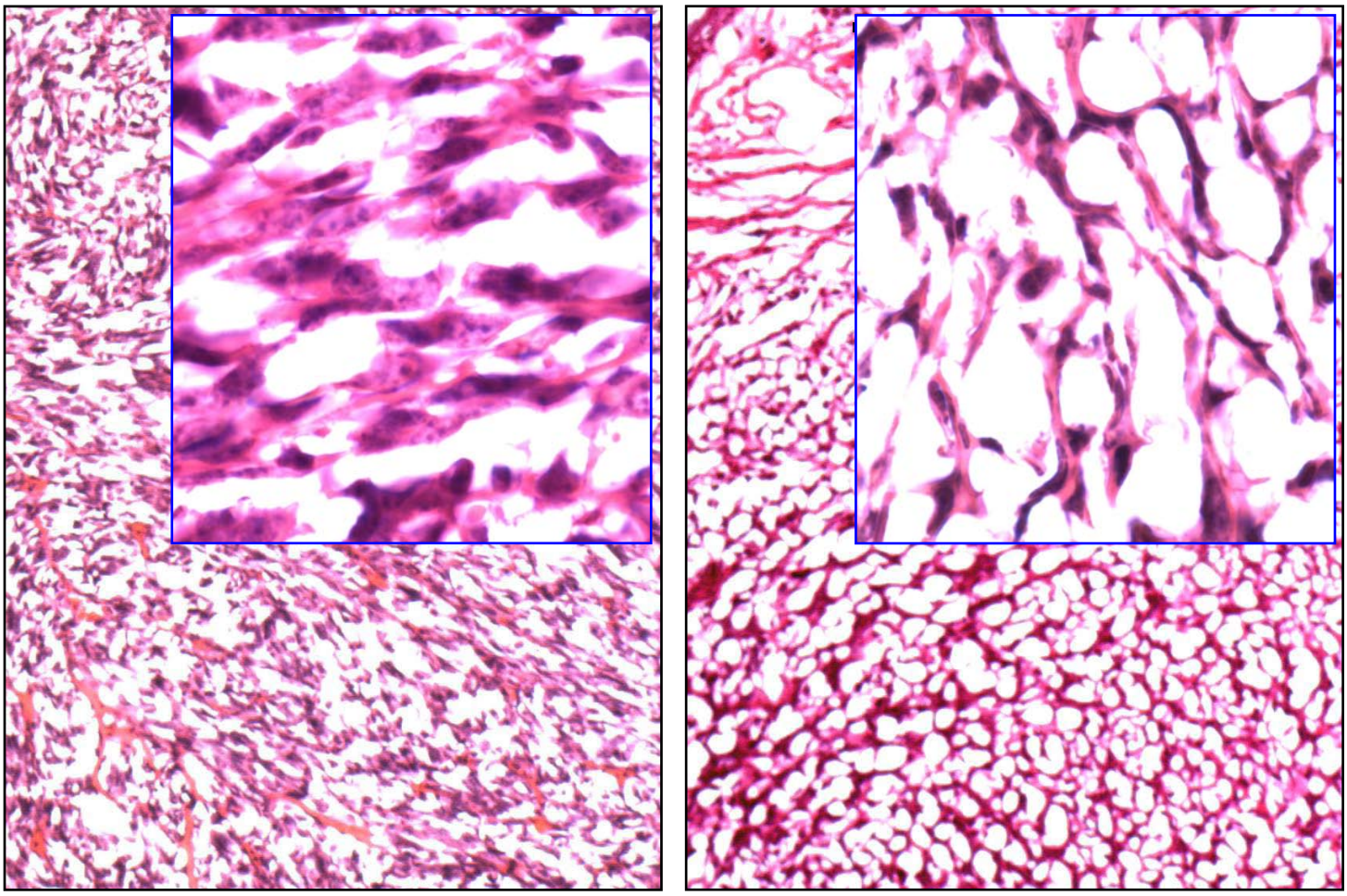

Jechlinger et al., Fig. S3

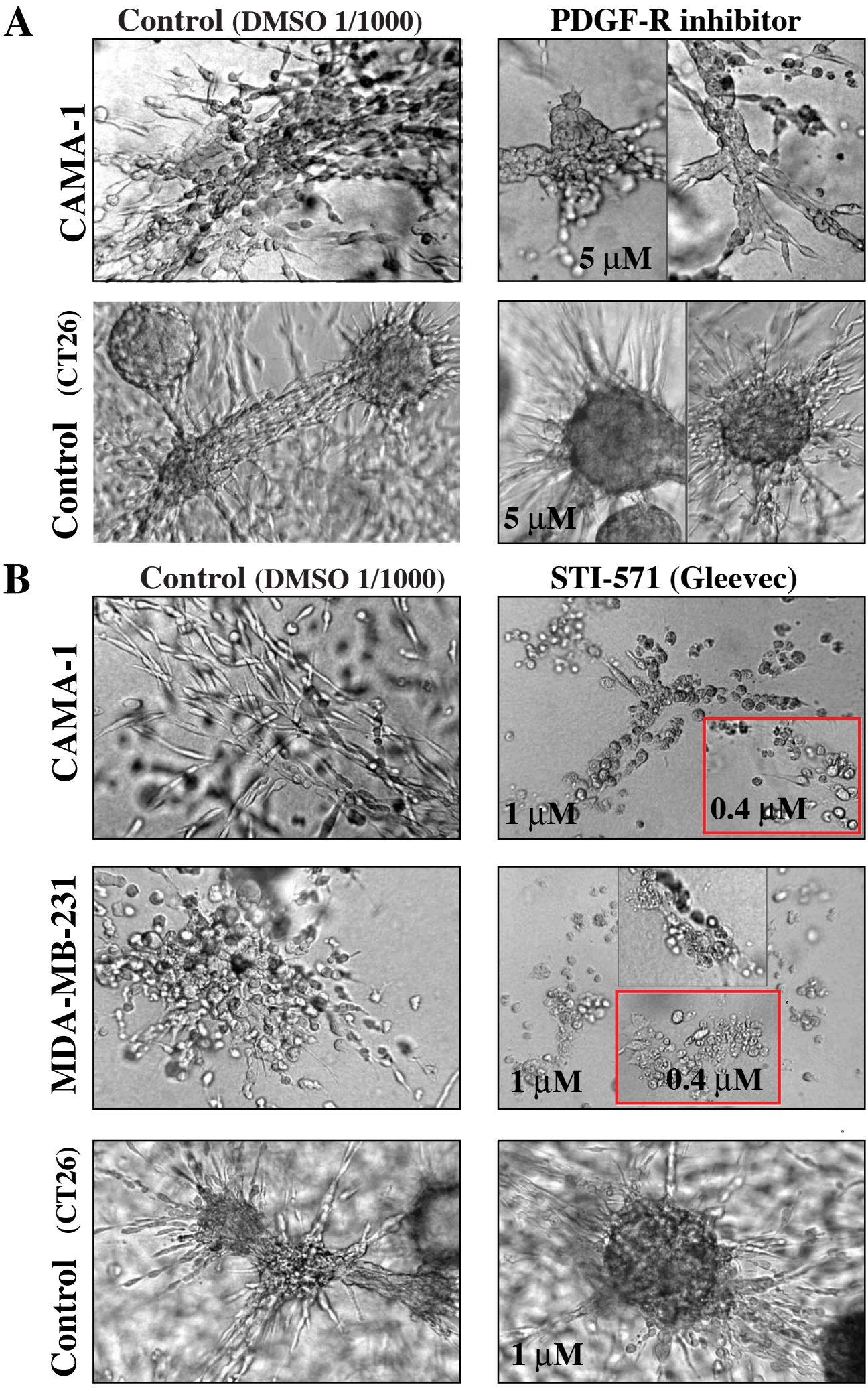

Jechlinger et al., Fig. S4